stationary slit selecting the beam that it is desired to record, and film, *F*, and interferometer, *SMA*, together traverse to and fro as indicated by the double-headed arrow. In Fig. 2.7.5.1, *S*, *M*, and *A* are the three equally thick wafers of the interferometer that remain upstanding above the base of the monolithic interferometer after the gaps between *S* and *M*, and *M* and *A*, have been milled away. The elements *S*, *M* and *A* are called the splitter, mirror, and analyser, respectively. The moiré pattern is formed between the Bragg planes of *A* and the standing-wave pattern in the overlapping $\mathbf{K}_0$ and $\mathbf{K}_h$ beams entering it. Maximum fringe visibility occurs in the emerging beam that the slit *Q* is shown selecting. A dislocation will appear in the moiré pattern whether the lattice dislocation lies in *S*, *M*, or *A*, provided $\mathbf{b} \cdot \mathbf{h} \neq 0$. Moiré patterns formed in a number of Bragg reflections whose normals lie in, or not greatly inclined to, the plane of the wafers, can be recorded by appropriate orientation of the monolith. By this means, it is easily discovered in which wafer the dislocation lies, and its Burgers vector can be completely determined, including its sense, the latter being found by a deliberate slight elastic deformation of the interferometer (Hart, 1972). Satisfactory moiré topographs have been obtained with an interferometer in a synchrotron beam, despite thermal gradients due to the local intense irradiation (Hart, Sauvage & Siddons, 1980).

Fig. 2.7.5.2 shows crystal slices (1), *ABCD*, and (2), *EFGH*, superposed and simultaneously Bragg reflecting in the Brádler–Lang (1968) method of X-ray moiré topography. The slices could have been cut from separate crystals. In the case when the Bragg planes of (1) and (2) are in identical orientation but have a translational mismatch across *CD* and *EF* with a component parallel to **h**, strong scattering occurs towards *Z* as focus, producing extra intensity at T' in the $\mathbf{K}_0$ beam TT'' and at R' in the $\mathbf{K}_h$ beam RR''. It is usual to record the moiré pattern using the $\mathbf{K}_h$ beam. Projection moiré topographs are obtained by the standard procedure of traversing the crystal pair and film together with respect to the incident beam *SO*. The special procedure devised for mutually aligning the two crystals so that $\mathbf{h}_1$ and $\mathbf{h}_2$ coincide within their angular range of reflection is explained by Brádler & Lang (1968). This method has been applied to silicon and to natural (Lang, 1968) and synthetic quartz (Lang, 1978).

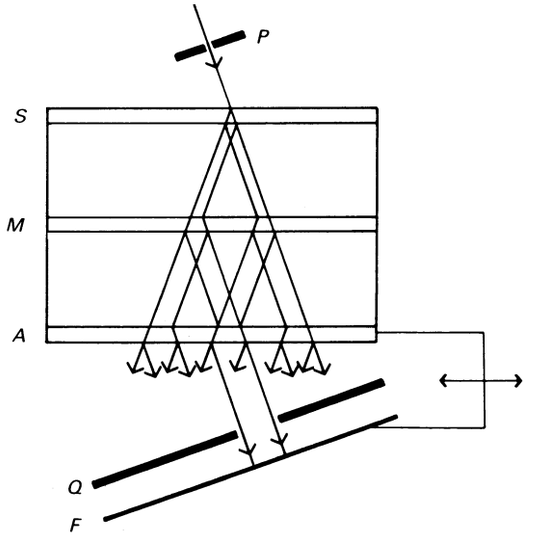

Fig. 2.7.5.1. Scanning arrangement for moiré topography with the Bonse–Hart interferometer.

2.7.5.2. *Real-time viewing of topograph images*

Position-sensitive detectors involving the production of electrons are described in Chapter 7.1, Sections 7.1.6 and 7.1.7, and Arndt (1986, 1990). Those descriptions cover all the image-forming devices that form the core of systems set up for 'live' X-ray topography. Here, discussion is limited to remarks on the historical development of techniques designed for making X-ray topographic images directly visible, and on the leading systems that are now sufficiently developed to be acceptable for routine use, in particular on topograph cameras set up at synchrotron X-ray sources. Two types of system became practicalities about the same time, that using direct conversion of X-rays to electronic signals by means of an X-ray-sensitive vidicon television camera tube (Chikawa & Fujimoto, 1968), and the indirect method using an external X-ray phosphor coupled to a multistage electronic image-intensifier tube (Reifsnider & Green, 1968; Lang & Reifsnider, 1969) or to a television-camera tube incorporating an image-intensifier stage (Meieran, Landre & O'Hara, 1969). These two approaches, the direct and the indirect, remain in competition. Developments up to the middle 1970's have been comprehensively reviewed by Hartman (1977). Since that time, Si-based, two-dimensional CCD (charge-coupled device) arrays have come into prominence as radiation detectors. They can be used for direct conversion of low-energy X-rays into electronic charges as well as for recording images of phosphor screens. As illustrated by Allinson (1994), four configurations employing CCD arrays for X-ray imaging can be considered: (i) direct detection by the 'naked' device; (ii) detection by phosphor coated directly on the CCD array; (iii) phosphor separate, and optically coupled to the CCD by lens or fibre-optics; and (iv) the addition to (iii) of an image intensifier

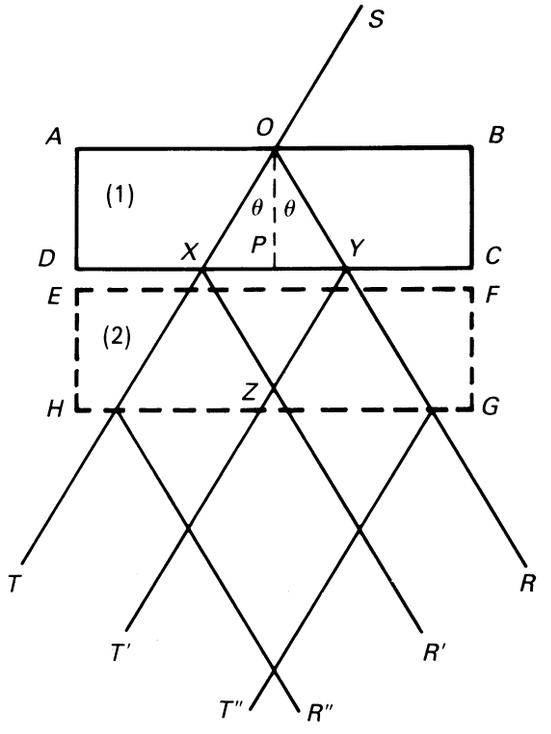

Fig. 2.7.5.2. Superposition of crystals (1) and (2) for production of moiré topographs. [Reproduced from *Diffraction and Imaging Techniques in Material Science*, Vol. II. *Imaging and Diffraction Techniques*, edited by S. Amelinckx, R. Gevers & J. Van Landuyt (1978), Fig. 21, p. 695. Amsterdam, New York, Oxford: North-Holland.]

or microchannel plate coupled to the phosphor screen. Consider first configuration (i). X-ray absorption efficiency in the active layer of silicon is near unity for radiations such as Cu $K\alpha$, and is not less than about 20% for Mo $K\alpha$ or Ag $K\alpha$. Since about one-third of the absorbed energy goes into electron–hole pair production, an absorbed 8 keV X-ray photon creates about 2000 pairs, a large number compared with a combined dark-current plus read-out noise level per photosite of a few tens of electrons r.m.s. Thus, single-photon counting is possible. Moreover, a cooled CCD can integrate the charge accumulated in each pixel for up to $\sim 10^3$ s. With pixel sizes in the range 10 to 30 μm square, and 1024×1024 (or 2048×2048) arrays in production, sensitive areas of 50 mm square, or greater, are available, sufficient for the majority of topographic applications.

For X-ray-sensitive TV-camera tubes, some major improvements in resolution and sensitivity have taken place since the first applications to X-ray topography of Be-windowed vidicons. Using the more sensitive 'Saticon' tube with incorporation of a 20 μm-thick Se–As target that provides good X-ray absorption efficiency, Chikawa, Sato & Fujimoto (1984) achieved a resolution as good as 6 μm at a modulation transfer function (MTF) of 5%. This betters that achieved with indirect systems or with standard-pixel-size CCD arrays used as direct detectors. The newer 'Harp' tube, which employs avalanche multiplication produced by a high field ($\sim 10^8$ V m^{-1}) applied across a 2 μm Se target to increase light sensitivity at least ten fold compared with the Saticon tube, has also been modified into a direct X-ray detector. Increasing the target thickness to 8 μm and adding an X-ray-transparent window provides satisfactory detector efficiency over a useful wavelength range (and the Se $K\alpha$-absorption edge at 0.098 nm causes absorption efficiencies for Cu $K\alpha$ and Mo $K\alpha$ to be similar, about 25%). The gain is sufficient for detection of single Cu $K\alpha$ photon-absorption events (at least for photons absorbed close to the target front, giving the maximum path for avalanche formation). A limiting resolution of about 25 μm (at MTF of ~33%) is exhibited (Sato, Maruyama, Goto, Fujimoto, Shidara, Kawamura, Hirai, Sakai & Chikawa, 1993), not yet as good as the 6 μm achieved with the Saticon tube. The rather small 6×9 mm sensitive areas of these camera tubes (when in standard '$\frac{2}{3}$ in' size) restricts their range of topographic applications as direct detectors compared with CCD arrays, but their amorphous Se targets are less likely to be degraded by X-radiation damage than crystalline-silicon CCD arrays. The latter do suffer degradation, but recover after treatment (Allinson, Allsopp, Quayle & Magorrian, 1991).

In the case of indirect systems, the lens or fibre-optic plate situated between phosphor and detector automatically protects the latter from radiation damage. Somewhat better resolution can be achieved by lens coupling than by fibre-optic coupling of phosphor to detector, but at the expense of loss of light-collection efficiency generally too great to be acceptable. In principle, magnification or de-magnification of the phosphor-screen image on the detector can be selected according to whether phosphor or detector has the better resolution, in order to maximize the system resolution as a whole. Phosphor resolution can be increased by diminishing its thickness below the value that would be chosen from consideration of X-ray absorption efficiency alone. Using a phosphor screen of Gd_2O_2S(Tb) only 5 μm thick, and lens-coupling it with tenfold magnification on to the target of a low-light-level television camera, Hartmann achieved a system resolution of about 10 μm (Queisser, Hartmann & Hagen, 1981), as good as any demonstrated so far with indirect systems.

The phosphors already used (or potentially usable) in real-time X-ray topography are inorganic compounds containing elements of medium or heavy atomic weight. They include ZnS(Ag), NaI(Tl), CsI(Tl), Y_2O_2S(Tb), Y_2O_2S(Eu), La_2O_2S(Eu) and Gd_2O_2S(Tb). Problems encountered are light loss by light trapping within single-crystal phosphor sheets, and resolution loss by light scattering from grain to grain in phosphor powders. Various ways of reducing lateral light-spreading within phosphor screens by imposing a columnar structure upon them have been tried. Most success has been achieved with CsI. Evaporated layers of this crystal have a natural tendency towards columnar cracking normal to the substrate. Then internal reflection within columns reduces 'cross talk' between columns (Stevels & Kühl, 1974). However, a columnar structure can be very effectively imposed on CsI films evaporated on to fibre-optic plates by etching away the cladding glass surrounding each fibre core to a depth of 10 μm, say. The evaporated CsI starts growing on the protruding cores, and continues as pillars physically separated and hence to a large degree optically separated from their neighbours (Ito, Yamaguchi & Oba, 1987; Allinson, 1994; Castelli, Allinson, Moon & Watson, 1994).

The drive to develop systems for 2D imaging of single-crystal or fibre diffraction patterns produced by synchrotron radiation that offer spatial resolution better than that within the grasp of position-sensitive multiwire gas proportional counters (say 100–200 μm) has produced several phosphor/fibre-optic/CCD combinations that with some modifications would be useful for real-time X-ray topography. Diffraction-pattern recording requires a sensitive area not less than about 50 mm in diameter, so most systems incorporate a fibre-optic taper to couple a larger phosphor screen with a small CCD array. Spatial resolution in the X-ray image cannot then be better than CCD pixel size multiplied by the taper ratio. In one system that has been fully described, this product is 20.5 μm × 2.6, and a point-spread FWHM of 80 μm on a 51×51 mm input area was realised without benefit from a columnar-structure phosphor (Tate, Eikenberry, Barna, Wall, Lawrance & Gruner, 1995). More appropriate for X-ray topography would be unit-magnification optical coupling of phosphor with a CCD array of not less than 1024×1024 elements and not more than 20 μm square pixel size. With such a combination, a system resolution of ~25 μm should be achievable; and at a synchrotron X-ray topography station at least one device offering resolution no worse than this should be available. There is a scope for both high-resolution, small-sensitive-area and lower-resolution, large-sensitive-area imaging systems in real-time X-ray topography. It has been shown possible to incorporate both types in a single topography camera for use with synchrotron radiation (Suzuki, Ando, Hayakawa, Nittono, Hashizume, Kishino & Kohra, 1984).

references